

**Alexandra M. Kuznetsova<sup>1,2\*</sup>, Georgy A. Baydakov<sup>1,2</sup>, Vladislav V. Papko<sup>1</sup>, Alexander A. Kandaurov<sup>1,2</sup>, Maxim I. Vdovin<sup>1,2</sup>, Daniil A. Sergeev<sup>1,2</sup>, Yuliya I. Troitskaya<sup>1, 2</sup>**

<sup>1</sup> Institute of Applied Physics of the Russian Academy of Sciences, 46 Ulyanov st., 603950, Nizhny Novgorod, Russian Federation,

\* **Corresponding author**; e-mail: alexandra@hydro.appl.sci-nnov.ru

<sup>2</sup> Nizhny Novgorod State University, 23 Gagarina av, 603950, Nizhny Novgorod, Russian Federation

# FIELD AND NUMERICAL STUDY OF THE WIND-WAVE REGIME ON THE GORKY RESERVOIR

**ABSTRACT.** The paper describes the study of wind-wave regime at the Gorky reservoir. A series of field experiments (carried out from May to October in 2012–2015) showed that the values of the drag coefficient  $C_D$  for a middle-sized reservoir in the range of moderate and strong winds are approximately 50 % lower than its values typical of the ocean conditions. The obtained parameterization of  $C_D$  was implemented in the wave model WAVEWATCH III to receive the correct wave forecasts for a middle-sized reservoir. Statistical distribution of the wind speeds and directions called for consideration of wind field heterogeneity over the Gorky reservoir. It was incorporated using the wind forcing from atmospheric model WRF to WAVEWATCH III. Homogeneous wind forcing from the experimental data was compared with heterogeneous wind forcing from WRF. The need for further improvement of the quality of wind and wave prediction is discussed.

**KEY WORDS:** reservoir, field experiment, simulation, wind-wave interaction, WAVEWATCH III, WRF

## INTRODUCTION

The study and the prediction of the wave regime in middle-sized reservoirs has both scientific and practical importance. First of all, waves on the water are a major source of erosion of the banks of reservoirs. A correct wave prediction determines the safety of inland navigation. In addition, the processes of momentum and heat and moisture exchange over the reservoir define microclimate of the adjacent areas.

The study of the wave regime of middle-sized reservoirs (with a linear size of 10–100 km) is also relevant because of the lack of the experimental data. Rare examples of these experiments are presented in [Atakturk and

Katsaros, 1999; Babanin and Makin, 2008]. In this paper we describe a series of the field experiments carried out by our research group on the Gorky Reservoir. The results of the field experiments demonstrated the need to consider a number of specific characteristics of the wave regime of middle-sized reservoirs that should be taken into account in the high-quality wave forecasts.

Usually, the numerical description of the waves on the middle-sized lakes and reservoirs is based on the empirical models: for example, in [Podubnyi, Sukhova, 2002] there is a block for the numerical description of the surface waves in the Rybinsk and Ivankovo reservoirs based on the empirical formulas, and in [Sutyryna, 2011], the wave regime on

the Bratsk reservoir was also studied using the empirical relationships. But the empirical relationships are based on the averaged characteristics, which can not be used for the prediction of the extreme wave conditions that are highly important for the operational meteorology. Therefore, it is necessary to use modern numerical wave forecast models. They are based on the numerical solution of spectra action balance equation. The models are classified by their treatment of the source terms (physical processes). Outdated first- and second-generation models use observed spectral shapes and sustained spectral energy levels to infer effects of physical processes. Modern third-generation models (WAVEWATCH III [Tolman et al., 2014], WAM [Gunter et al., 1992], SWAN [SWAN team, 2006]) parameterize all physical processes explicitly, without imposing spectral shapes or energy levels. These models describe the evolution of a 2D wave spectrum under the impact of wind-wave interactions, dissipation, nonlinear wave-wave interactions, and in the case of shallow water, some of them also take into account the influence of the bottom friction, depth-induced breaking and triad wave-wave interactions.

It should be noted that the third-generation numerical models are adapted to the ocean conditions. However, the wave models were used successfully on large lakes. WAVEWATCH III was successfully used for the wave forecasts on the Great Lakes in the USA [Alves et al., 2011]. In addition, WAVEWATCH III and SWAN were applied successfully to the Caspian Sea and Lake Ladoga for wind and waves hindcast [Lopatoukhin et al., 2004]. Recently, the first results of the use of WAM to predict the surface waves in a middle-sized water body were obtained [Hesser, 2013]. We have chosen WAVEWATCH III model for the simulation of surface waves on middle-sized reservoirs, because this model considers the largest number of interactions available in the current model versions.

Thus, for the WAVEWATCH III application to the conditions of the middle-sized reservoir, the tuning of the model is required. The

tuning should be carried out in two steps: the adjusting of the wind input source term and the adjusting of the "collision integral." This adjusting is caused by the specific characteristics of the waves at small fetches of a middle-sized reservoir: the wind input, which is proportional to the relation of the friction velocity (or 10 m wind speed) to the phase wave velocity [Tolman et al., 2014] is more intense, as well as a stronger non-linearity is caused by steeper waves. The dissipation due to wave breaking remains unchanged. The first step of the tuning was implemented in [Kuznetsova et al., 2016 a].

In this work, the tuning implemented in [Kuznetsova et al., 2016 a] was used to study the ways to set the wind forcing. In the previous works [Kuznetsova et al., 2016 a, b], the wind speed was assumed to be homogeneous over the entire area of the reservoir due to the lack of the sufficient experimental data, and was obtained from the experimental measurements that consider temporal variability. This assumption is a source of possible errors in the numerical experiment. Consideration of the high spatial variability is a challenging task. To solve it, it is possible to use atmospheric models of high spatial resolution, for example, atmospheric model Weather Research & Forecasting (WRF). This method of the wind forcing characterization was realized, for example, in [Alves, 2014]. This paper presents the use of the wind forcing from WRF to WAVEWATCH III for middle-sized reservoirs.

## METHODS OF THE FIELD EXPERIMENT AT THE GORKY RESERVOIR

Field measurements were carried out from May to October in 2012–2015 in the waters of the Gorky reservoir which is formed by the dam of the Nizhny Novgorod hydroelectric station near the town of Gorodets on the Volga River. At the normal water level, it spans 430 km from the Rybinsk dam to the Nizhny Novgorod hydroelectric station dam, and its maximal width is 26 km. The water surface area is 1591 km<sup>2</sup>, the total volume

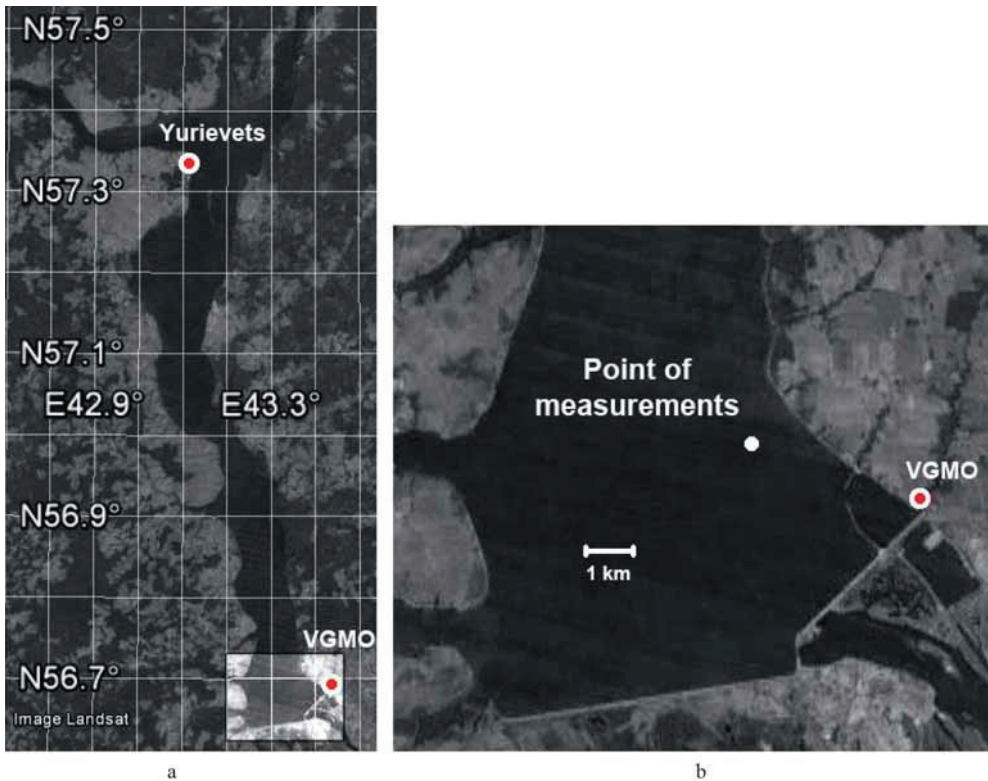
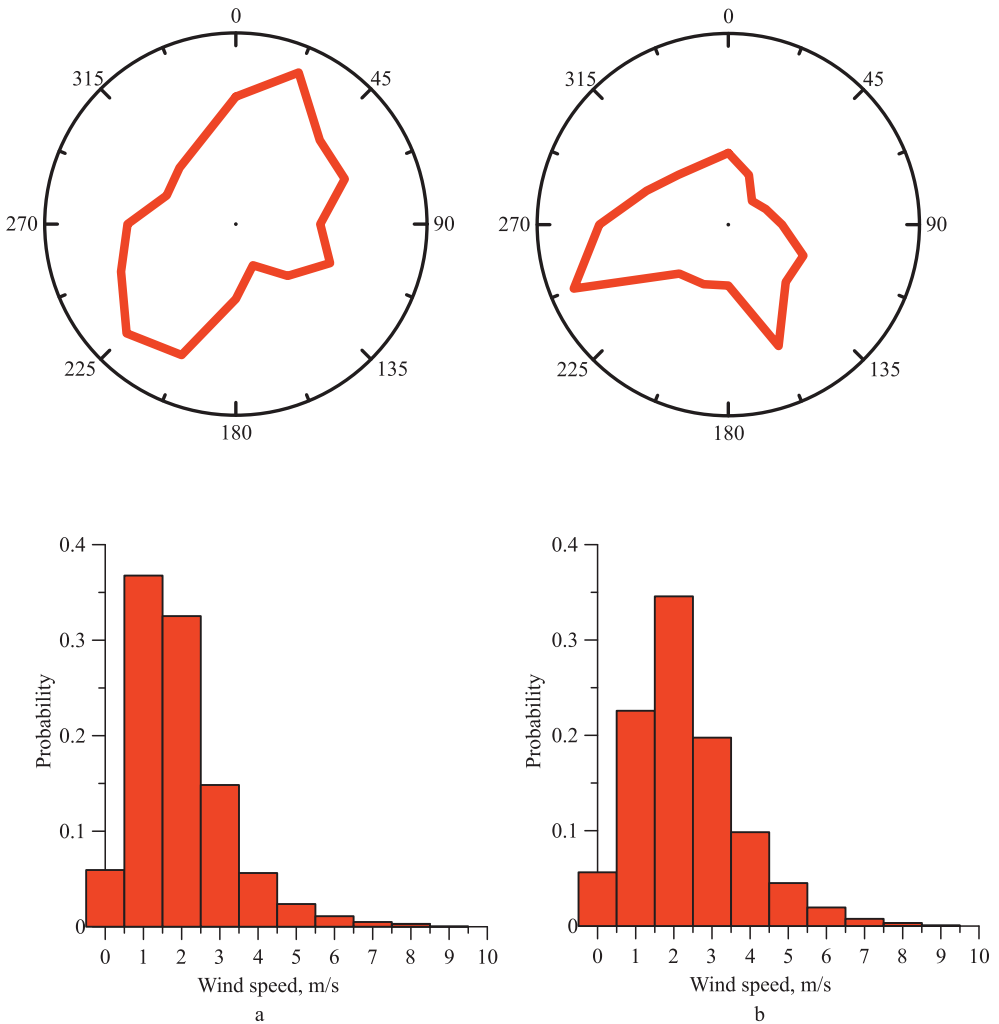


Fig. 1. a) The Gorky reservoir (Google Earth data); b) Zoom view of the measurements area. Red dots in white circles show the weather stations: Volzhskaya (VGMO) and Yurievets.

is  $8.8 \text{ km}^3$ , the useful volume is  $2.8 \text{ km}^3$ , and the useful volume of the navigational prism is  $0.6 \text{ km}^3$ . According to the hydrological regime and navigability, the reservoir is divided into three sections – river, lake, and river and lake. Measurements were carried out in the southern part of the lake area of the reservoir (Fig. 1). The lake area is 97 km from the Elnat River mouth to the Nizhny Novgorod hydroelectric station dam. The width of this part of the reservoir varies from 5 to 14 km, and only near the Puchezh city, it is 3 km. The depths of the main ship channel varies from 4.5 to 20 m, and in the study area, it varies from 9 to 12 m depending on the season and the point of measurement. Throughout the lake part of the reservoir, the right bank is high and sometimes steep. The left bank is low and flat almost everywhere; but near the Sokolskoye village and in the area extending from the city of Chkalovsk to the Nizhny Novgorod hydroelectric station dam, the bank is high and steep.

Fig. 2a shows the distribution of wind speed and direction measured at Volzhskaya weather station (Gorodets) close to the field study area. The distribution was based on the data for the navigational period (May 10 – October 31), 2010–2015. Despite the notable selected wind direction, the range of possible directions is rather wide. The elongated shape of the reservoir allows studying wind and waves of different fetches. Volzhskaya is located on the high bank (about 15 meters above the water level) and the values of the wind velocity at the shore are very different from those over the water area: the wind speed over the water area is up to two times higher. Fig. 2b shows the distribution of wind speed and direction measured at the Yurievets weather station at the same intervals. The difference between the distributions obtained from the two weather stations shows significant spatial inhomogeneity of the wind above the reservoir and, consequently, it is necessary



**Fig. 2. Statistical distribution of the wind directions (top graphs) and wind speeds (low graphs) averaged over 2010–2015 during the navigational period (from May 10 to October 31): a) Volzhskaya, b) Yurievets.**

to measure wind and wave characteristics at different points of the reservoir in order to determine the accurate prediction or statistical parameters of wind and waves.

The field studies include measurements of the wind velocity profile, surface waves, profiles of water and air temperature, and current velocity profile (see similar measurements in [Bakhanov et al., 2011]), as well as the measurement of turbulent air flow characteristics (see similar measurements in [Bogatov et al., 2014]) and in the water column. The measurements were carried out from a vessel (Fig. 3 a) using the author's

original buoy station (Fig. 3 b, c) based on the oceanographic Froude buoy station.

On the board of the vessel, an ultrasonic profiler of the current velocity ADCP (Teledyne RD Instruments), similar to that used in [Bakhanov et al., 2011], a high-frequency ultrasonic three-gauge wind speed HS-50 (sample rate is 50 Hz) (Gill Instruments) (see [Bogatov et al., 2014]), and CTD-probe (see results in [Ivanov et al., 2015]) were located.

The buoy represents a mast semi-submerged in the water and held in a vertical position by



**Fig. 3. a) Vessel on the Gorky reservoir. b) View of the operating state of the Froude buoy. c) Schematics of the Froude buoy.**

the float near the surface and by the load at a depth (Fig. 3 b, c). The total length of the mast is 12 m, the length of the topside is 5.3 m. The resonant frequency of vertical oscillations is 0.25 Hz, which corresponds to a wavelength of 25 m. On the buoy's mast, 4 ultrasonic speed sensors WindSonic (Gill Instruments) were located at heights of 0.85 m, 1.3 m, 2.27 m, 5.26 m. The fifth sensor was located on the float tracking the waveform for measuring the wind speed in the close proximity to the water surface. The distance from the float to the buoy's mast is 1 m, and the height of the wind speed measurement zone is 10 cm from the water surface. The buoy was also equipped with air temperature sensor (at heights of 0.1 m [float], 0.85 m, 1.3 m), water temperature sensor, and three-channel string wave gauges, which allowed us to retrieve the waves space-time spectra.

WindSonic is a two-component ultrasonic sensor with a 4 % measurement accuracy and velocity resolution of 0.01 m/s. Operating range of wind speed measurements 0–60 m/s includes measurements in calm conditions. Resistive temperature sensors measure the environmental temperature with resolution of 0.01 °C and a 3 % measurement accuracy. The wave gauge consists of three pairs of resistive wire sensors, located at the vertices of an equilateral triangle with a side of 62 mm, the

data sampling rate is 100 Hz. The system allows estimating parameters of the wave, which length exceeds the double distance between the sensors ( $k_{\max} \approx 0,5^{-1}$ ). The algorithm of the processing of the signals received from the devices uses the Fourier transform and is described in detail in [Troitskaya et al., 2012] (a similar algorithm which uses the wavelet transform is described in [Donelan et al., 1996]).

The particular attention in the study was paid to the determination of the dependence of the drag coefficient on the wind speed  $C_D(U_{10})$  (see, for example, [Troitskaya et al., 2012]), which defines the momentum flow from the wind to the waves. The dependence  $C_D(U_{10})$  is rather well studied for weak and moderate winds in the open ocean, and currently the great attention is paid to the wind-wave interaction under hurricane winds. However, the conditions of small and middle-sized water bodies are substantially different from those of the ocean (small fetches resulting in steep waves, and shielding of wind by the banks), and therefore it is fair to expect different wind-wave regime in these conditions. For example, the results obtained in [Atakturk and Katsaros, 1999; Babanin and Makin, 2008] show features of wind-wave regime in the conditions of inland waters.

## RESULTS OF THE FIELD EXPERIMENT

The field study included 44 experiments in a wide range of wind speeds (Fig. 4 a) in the point of measurement. It should be noted that the significant wave height is greatly influenced not only by wind speed, but also by its direction. Due to the small size of the vessel used for the field experiment, the measurements could not be carried out in heavy seas, so the direction of the observed wind speeds  $U_{10}$  with values more than 8 m/s is not north. This stipulation has a significant impact on the distribution of the measured waves heights  $H_S$  (Fig. 4 b) and of the spectral peaks  $f_p$  (Fig. 4 c).

An important feature which sets this study apart from the similar studies (see [Ataturk and Katsaros, 1999; Babanin and Makin, 2008]) is the use of a lower mobile speed sensor tracking the waveforms (see [Kuznetsova et al., 2016 a]). The value of drag coefficient  $C_D$  is determined by profiling [Kuznetsova et al., 2016 b], and the impact of the data from different horizons on the resulting approximation of the wind speed profile is analyzed. Fig. 5a shows the comparison of the retrieved relationships  $C_D(U_{10})$  for two combinations of speed sensors: with the use of the lower sensor and without it, as well as the results presented in [Ataturk and Katsaros, 1999; Babanin and Makin, 2008], and oceanic parameterization [Fairall et al., 2003]. The values  $C_D(U_{10})$  are higher and closer to the results of [Ataturk and Katsaros, 1999; Babanin and Makin, 2008; Fairall et al., 2003]

without the use of the lower sensor while the use of the lower sensor demonstrates lower values of the drag coefficient. Fig. 5b shows a comparison of the retrieved dependencies  $C_D(U_{10})$  with either two lower only or all five sensors. The use of two sensors only demonstrates significant differences in the retrieving of winds in the range of weak winds.

These results can be interpreted by the deviation of the wind speed profile shape from the logarithmic one. This difference is probably due to the stratification of the atmospheric surface layer as well as to the nonstationary wind, as the lower part of the profile quickly adapts to the changing conditions of the surface waves, wherein the parameters of the air flow determine the momentum transfer from the wind to the waves exactly at the water-air boundary.

Thus, it has been demonstrated that the use of the lower sensor, in particular the use of the two lower sensors only, significantly affects the results of the measurement. To determine the accuracy of the measured dependence  $C_D(U_{10})$ , it was used in the numerical simulation of wind waves in the framework of WAVEWATCH III. To do this, the experimental data were fitted (Fig. 5b) with the function:

$$C_D = 0.00124U_{10}^{-1} + 0.00034 + 0.000049U_{10}. \quad (1)$$

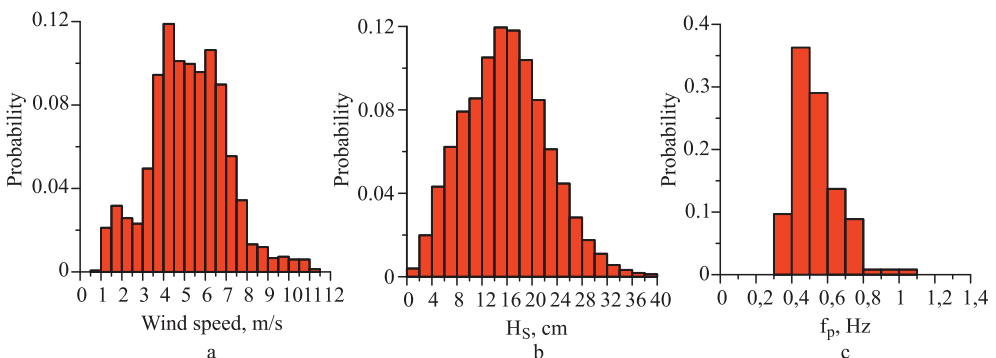


**Fig. 4. The statistical distribution of the values measured during the experiment:**

a) wind speed, b) significant wave height, c) peak frequency.

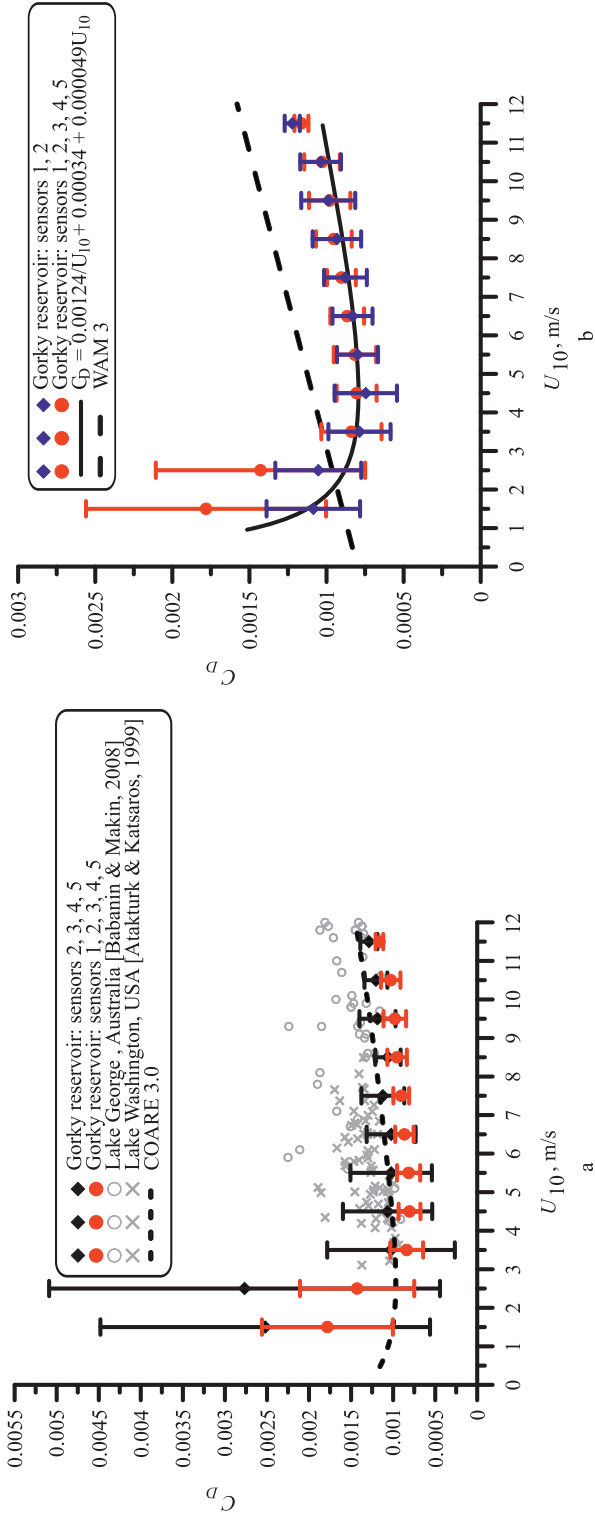


**Fig. 5. Comparison of the retrieved dependences  $C_D(U_{10})$ :**

a) with and without the lower sensor: black diamonds denote the binning of data with the lower sensor (with the standard deviation as the error gates), red solid circles denote the binning of the data without the lower sensor (with the standard deviation as the error gates), gray crosses are the results of the field experiment [Babanin and Makin, 2008], gray circles are the results of the field experiment [Atakturk and Katsaros, 1999], dashed line is the empiric ocean parameterization COARE 3.0; b) using two and five sensors: red solid circles are the binning of the five-sensors data (with the standard deviation as the error gates), blue diamonds are the binning of the two-sensors data (with the standard deviation as the error gates), solid line is an approximation of the obtained data by a function  $C_D = 0.00124 \cdot U_{10}^{-1} + 0.000049 \cdot U_{10}$ , dashed line is the WAM 3 parameterization [Wu, 1982].

## SIMULATION

To apply the wave prediction model WAVEWATCH III to the conditions of a middle-sized reservoir, the tuning of the model was needed. The reasons and steps for the tuning are discussed in detail in the introduction.

In this study, we used the adapted to the conditions of an inland water body WAVEWATCH III model [Kuznetsova et al., 2016 a], where adjustments of the wind input and a number of other modifications in the WAVEWATCH III code were implemented, including: in the open code, the minimal value of a significant wave height  $H_S$  was adjusted; then, for the reservoir description, the topographic grid of the Gorky reservoir with dimensions 72×108 and increments of 0.00833° was used. The grid was taken from the NOAA data "Global Land One-Kilometer Base Elevation (GLOBE)" (Fig. 6a). It should be noted that there is no open-source reliable information about the bathymetry of the considered area; the existing navigational maps have not been digitized. This is a

subject for another study. Although these navigational maps showed that the depth was sufficient to consider it deep water. In addition, the observed wavelength in the field experiments is less than 4.5 m, and therefore, the exact bathymetry was not considered in calculations, and depth was chosen to be 9 m. The frequency range was changed to 0.2–4 Hz in accordance with the experimentally observed range, which was split in 31 frequencies in the simulation and was modeled by a logarithmic formula for the frequency growth  $\sigma_N = (\delta)^{N-1} \sigma_1$ , where the growth rate was determined to be  $\delta = 1.1$  in accordance with the recommendations of [Tolman et al., 2014]; 30 angular directions of the wave field were considered. The waves in the reservoir were simulated for a given Gaussian initial seeding for different wind input parameterizations using the specified topographic data, wind speed and direction, and water-air temperature difference.

Typical values of wind speeds for the calculations are weak and moderate wind

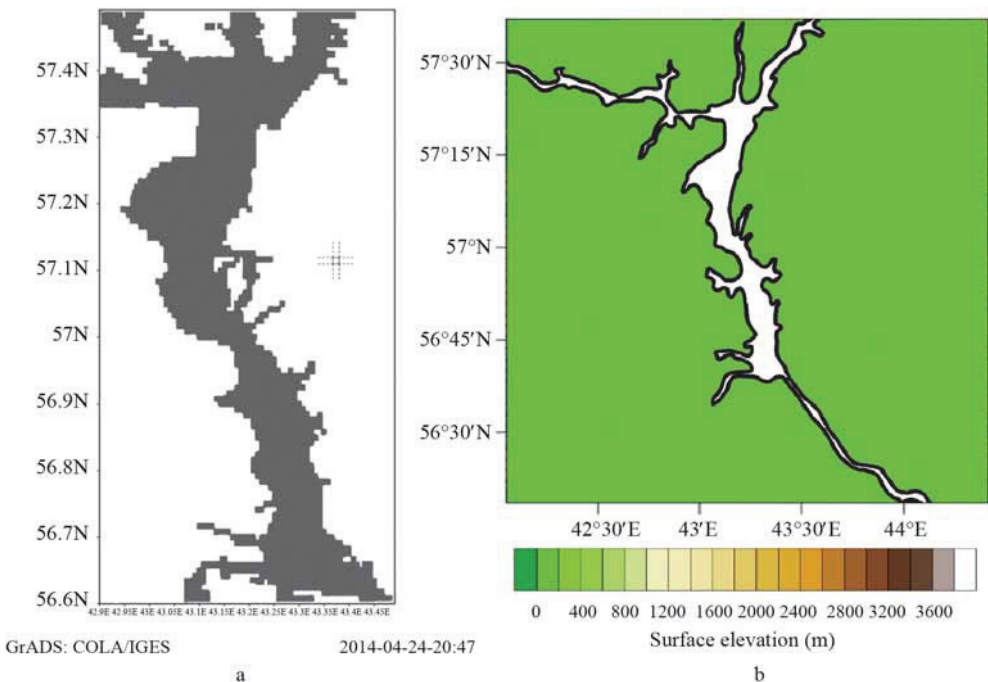


Fig. 6. Topographical grid of the Gorky reservoir in a) WAVEWATCH III, b) WRF. Computational cell with a size of 0.00833° is shown.



( $U_{10} = 1 \div 9$  m/s) of different directions. Two types of wind input data were studied. First, wind forcing was set as the value of wind speed measured in the experiments and assumed homogeneous over the entire surface of the Gorky reservoir; variability in time was taken into account. The simulation was held with input data updated every 15 minutes, measured in the field experiment: 10 m wind speed and direction, the water-air temperature difference. In practice, to simulate wind waves on the surface of the seas and oceans, the reanalysis data is typically used as a wind forcing. It has a spatial variability that can help to simulate the wave regime more accurately. In the middle-sized inland waters, this approach is not applicable because of its too low spatial resolution ( $2.5^\circ$ ). In addition, the reanalysis data are more precise the more data assimilation occurs in this area. In the studied area there are only two weather stations (Volzhskaya and Yurievets), but they are on the coast, and the wind speed on the coast is different from that over the waters of the reservoir. In this regard, the use of the reanalysis data in a simple form is not correct. This assumption of the homogeneity of the wind forcing over the pond can be a source of errors in a numerical experiment, because the wind field is expected to be heterogeneous, and such factors as the elongated shape of the reservoir and the high banks can lead to a significant spatial variability of the wind field. The heterogeneity of the wind field over the reservoir was supported by the field study of wind conditions over the entire water area (see Fig. 2). Thus, the second method of the wind forcing setting in the simulation was used. It was realized taking considering the spatial variability of the wind field using the wind forcing from the atmospheric model WRF.

To apply WRF to the calculation of the wind field over the Gorky reservoir, the following steps were undertaken. In WRF preprocessing system, the preprocessing of the data to prepare the input to the real program for real-data simulations was realized. For the geogrid module, the recommended geographical data for the lakes description "modis\_lakes"

for four nested domains in the studied region was used. The minimal cell size of the fourth nested domain was 30 arcseconds (it is equivalent to the cell size of the topographical data used in WAVEWATCH III  $0.00833^\circ$ ) (Fig. 6b). These data were used to describe the domains and to interpolate the static geographical information for the given grid. To describe the current weather situation, the meteorological data "NCEP Final Analysis (FNL from GFS) (ds083.2)" with 1 degree resolution was loaded. It was updated every 6 hours and was extracted from the GRIB format using the ungrib program. Metgrid program produced a horizontal interpolation of the extracted meteorological data on the domains grid. The simulations were conducted on the Yellowstone supercomputer, Boulder, USA [Computational and Information Systems Laboratory, 2012].

Simulation was carried out in two ways: firstly, in the framework of the ocean parameterization WAM 3, which uses a linear dependence of the  $C_D$  on  $U_{10}$  [Wu, 1982], and secondly, with our proposed parameterization of  $C_D(1)$  in the wind input source term WAM 3. The difference of parameterizations  $C_D(U_{10})$  is shown in Fig. 5b. For the wind speeds of up to 2.5 m/s, the  $C_D$  values from the field experiment lie above the  $C_D$  values given by the ocean parameterization, and for the wind speeds greater than 3 m/s, they lie below.

## RESULTS OF THE SIMULATION AND DISCUSSION

The comparison is made for the following WAVEWATCH III output: significant wave heights and mean wave periods. Both in the model and in the processing of the experimental results, the calculation of  $H_S$  was performed by the formula:

$$H_S = 4\sqrt{E}. \quad (2)$$

The calculation of mean wave period  $T_m$  was performed by the formula:

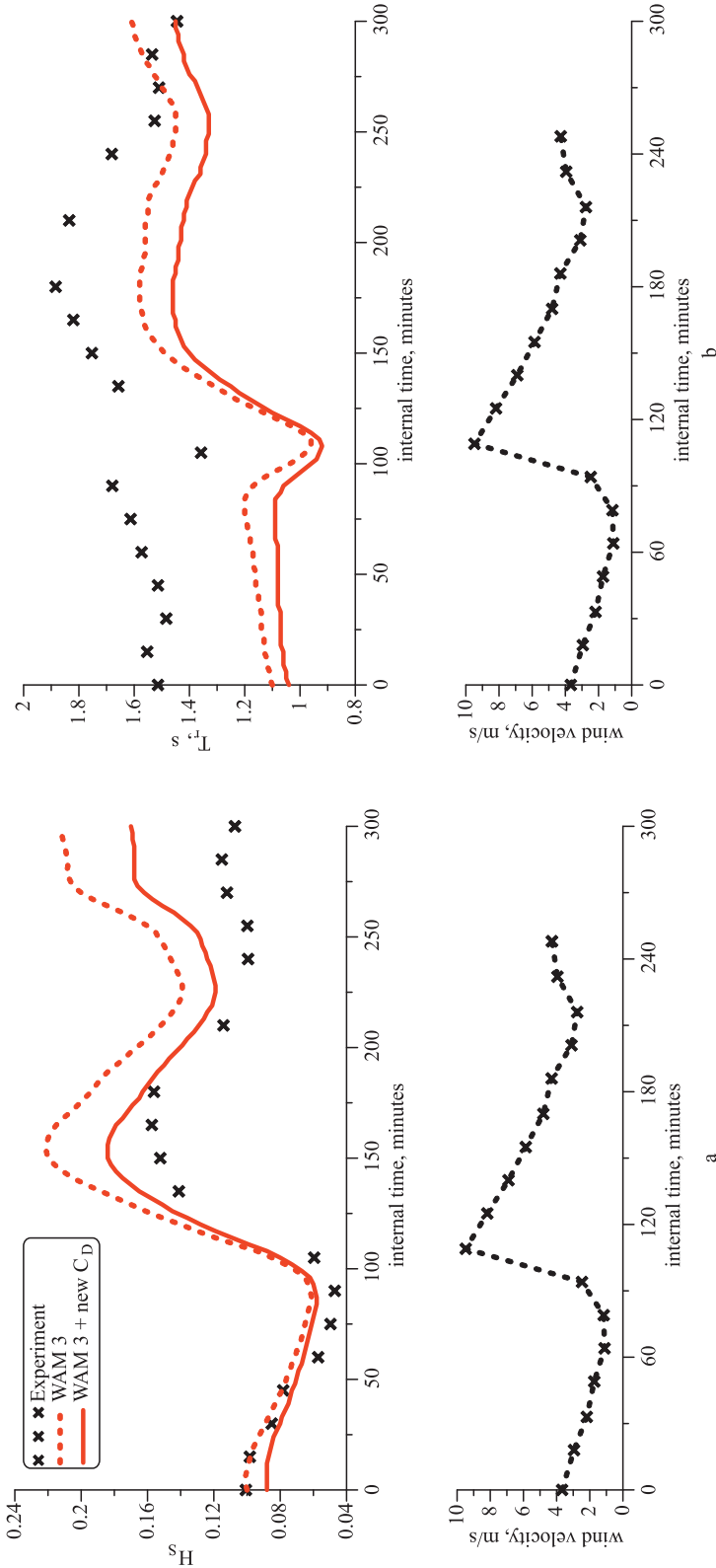


Fig. 7. On the top plots: the retrieved values of a)  $H_s$  and b)  $T_{ms}$  obtained both from the field experiment (crosses) and from the numerical experiment (red dashed line for the WAM 3 parameterization, red solid line for the WAM 3 parameterization with new  $C_D(U_{10})$ ). On the lower plots: the measured values of the wind used in the simulation.

$$T_m = T_{m0,-1} \left( \int_{f_{\min}}^{f_i} E(f) df \right)^{-1} \int_{f_{\min}}^{f_i} E(f) f^{-1} df. \quad (3)$$

All the data were obtained at the point corresponding to the point of the observations.

### *Wind forcing from the experimental data*

When the wind forcing is set as the constant value of the wind speed measured in the experiment, the output data from the simulation were averaged over the interval of 15 minutes to correspond with the similarly averaged data from the field experiment.

Fig. 7 shows the results of the modeling and field measurements for the test day 13.06.13 using the ocean model WAM 3 and new parameterization  $C_D(U_{10})$  within WAM 3. The lower plots show the measured values of the wind used in the simulation, the plot on the top shows a change for the retrieved values of  $H_S$  and  $T_m$ , obtained both from the field and numerical experiments. As it can be seen from Fig. 7, usually the values of the significant wave height in simulations with WAM 3 parameterizations are overestimated. The use of the proposed parameterization  $C_D(U_{10})$  reduces the standard deviation of  $H_S$  for WAM 3 parameterization compared to the field experiment. This is the expected result, as in the numerical experiment with the use of new parameterization of  $C_D$ , the wave growth rate was defined more precisely, which means that the amount of energy entering the system was simulated more accurately.

However, the top graphs of Fig. 7b show that the prediction of mean wave periods has a significant discrepancy with the measured ones, and the use of the new parameterization of  $C_D(U_{10})$  does not have a sufficient impact. Perhaps, this is due to the fact that the tuning of WAVEWATCH III to marine environment was reflected not only in the function of the wind input, but also in taking into account the specific parameters of numerical nonlinear scheme DIA [Hasselmann and Hasselmann,

1985; Hasselmann et al., 1985], because nonlinear processes are responsible for the redistribution of the energy received from the wind in the spectrum. WAVEWATCH III considers the wave characteristics of marine and ocean conditions, which have a lower slope compared to the waves on the middle-sized inland waters. The coefficients of proportionality in the scheme DIA were adjusted to the sea conditions. Steeper waves of a middle-sized reservoir may require a different adjustment of parameters corresponding to a situation with stronger non-linearity, which should lead to a more rapid frequencies downshift. Consequently, mean wave periods will decrease. At the same time, we can expect that such a tuning of the numerical nonlinear scheme should not affect the quality of the predictions of  $H_S$ , which indicates the amount of energy received by the system, but should lead to a better prediction of mean wave periods. This hypothesis will be tested in the subsequent numerical experiments.

The advantages of the use of the proposed parameterization  $C_D(U_{10})$  are described in detail in [Kuznetsova et al., 2016 a].

### *Wind forcing from WRF*

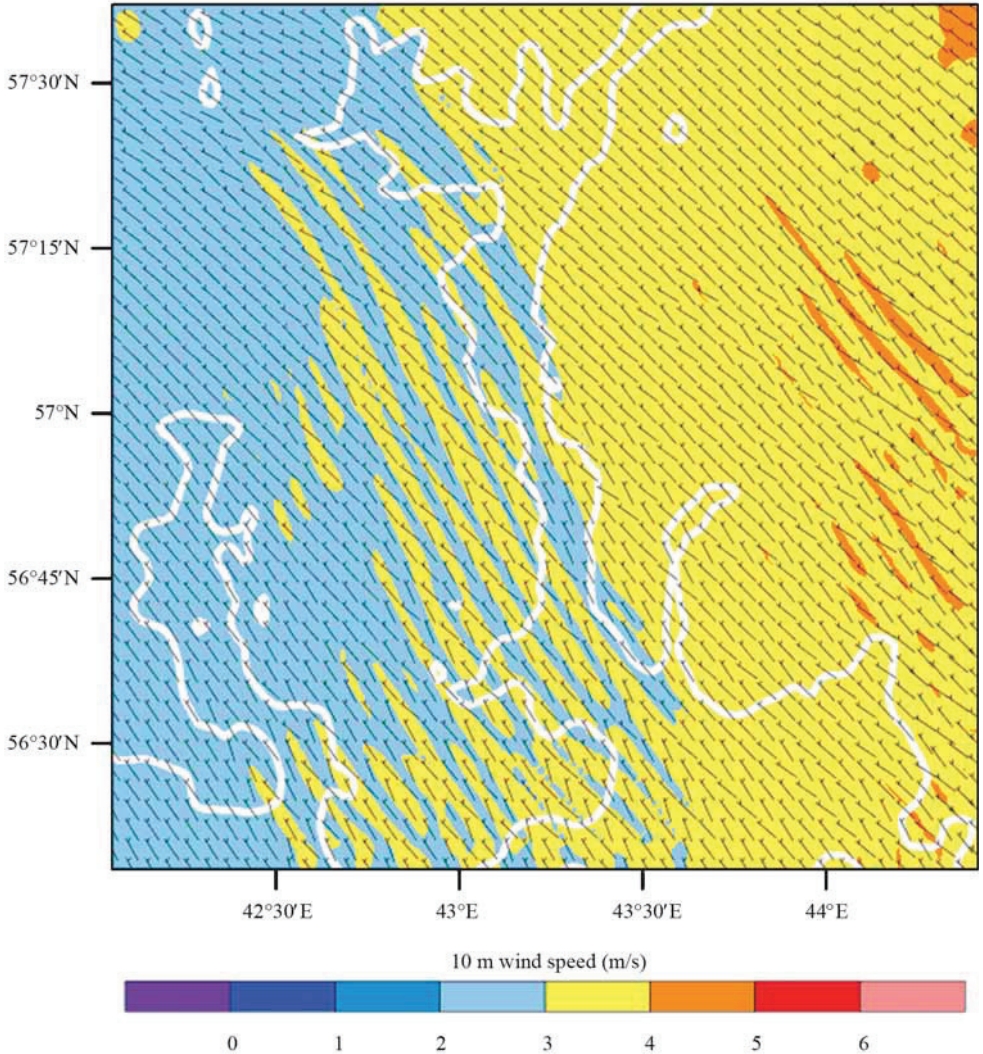
The use of WRF wind forcing was the next step in improving the wave forecast and eliminating the possible causes of errors in the numerical experiment. The WRF application to the area containing the Gorky reservoir showed the significant spatial variability of the wind over the water area. The results obtained in the simulation for the test day 13.06.13 are presented in Fig. 8.

The distribution of the wind over the water area of the Gorky reservoir (Fig. 8) is heterogeneous both in the value (indicated by color), and in the direction (indicated by the direction of the segment). However, the values of the wind speed are much lower than those measured in the field experiment in the test day 13.06.13. This is also supported by the lower graphs in Fig. 9, which show the value of the wind measured in the experiment

### REAL-TIME WRF

Init: 2013-06-12\_06:00:00  
Valid: 2013-06-13\_10:00:00

Terrain Height (m)  
10 m wind speed (m/s)  
Wind (m s - 1)



OUTPUT FROM WAF V3.6 MODEL  
WE = 133; SN = 133; Levels = 30; Dis = 1.1111 km; Phys Opt = 3; PBL Opt = 1; Cu Opt = 0

Fig. 8. The distribution of the wind over the water area of the Gorky reservoir in the test day 13.06.13, WRF simulation.

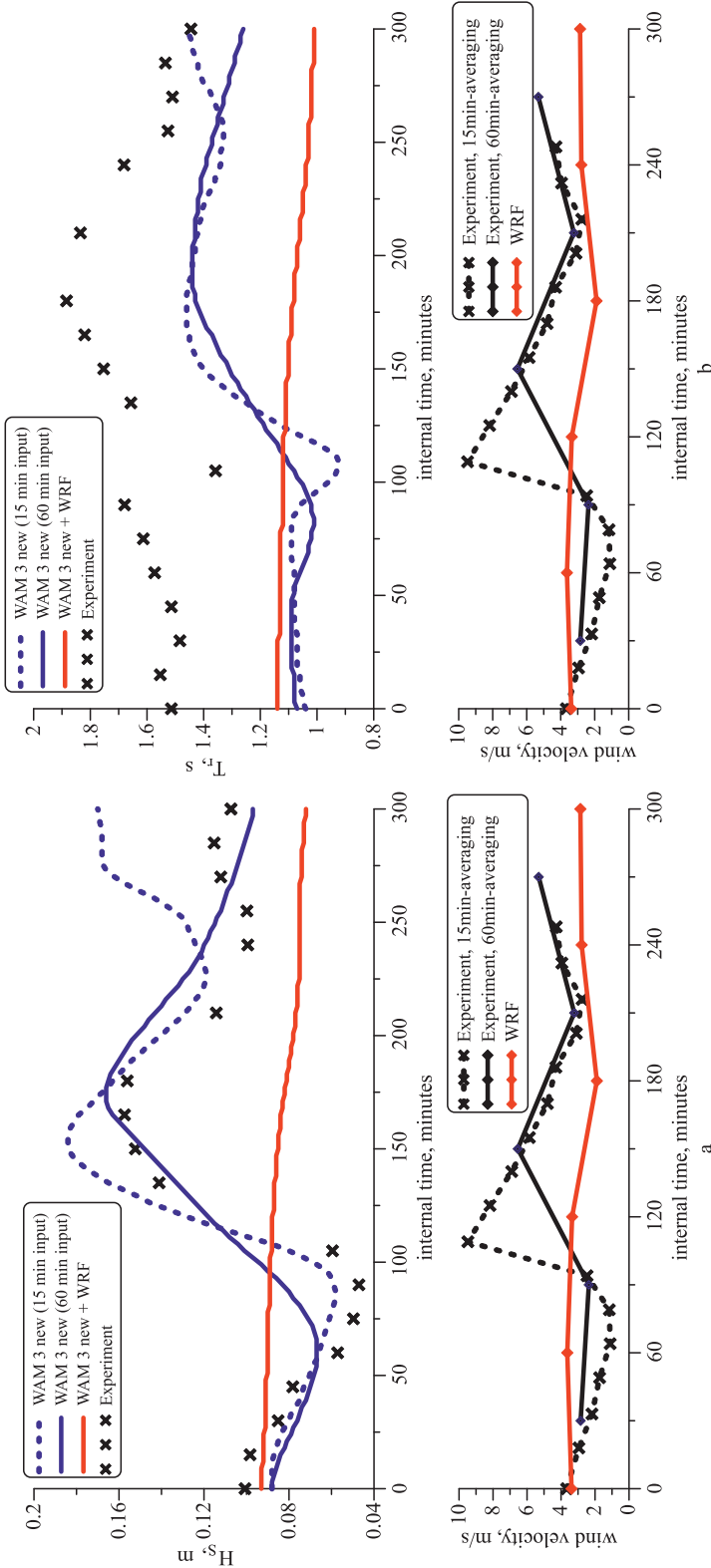


Fig. 9. Top plots: a)  $H_s$  and b)  $T_m$  for: WAM 3 with new  $C_D(U_{10})$  with wind forcing from the experiment averaged over 15 minutes (blue dashed line), WAM 3 with new  $C_D(U_{10})$  with wind forcing from the experiment averaged over 60 minutes (blue solid line), WAM 3 with new  $C_D(U_{10})$  with WRF wind forcing (red solid line). Lower plots: wind measured in the experiment and averaged over 15 minutes (dashed black line), wind measured in the experiment and averaged over 60 minutes (black line), wind from WRF, averaged over 60 minutes (red line).

and averaged over 15 minutes (dashed black line) and over 60 minutes (black line) for the convenience of the comparison with the wind from WRF, which was also averaged over 60 minutes (red line).

We associate this inaccuracy of wind prediction in WRF model with several factors. First, with a small amount of data assimilated in the test area. As it was discussed in section "Simulation," there are only two weather stations (Volzhskaya and Yurievets) in the study area, and they are located on the coast, where the wind speed is significantly different from that over the waters of the reservoir. Consequently, the data from the additional sources (e.g., private weather stations) along the perimeter of the pond is needed. Installation of the private weather stations is part of the future study.

Second, we associate this inaccuracy with the insufficient precision of the geographical data resolution. With the increase of the precision, the inclusion of the Large Eddy Simulation (LES) unit will be possible, and this unit will help to create highly accurate forecasts incorporating the calculation of turbulent flows.

Fig. 9 shows that the change of the wind averaging from experimental data over 15 minutes and over 60 minutes, of course, affects the dependence of the wind on time. However, on average, the wind given by the experiment was higher than the wind, given by WRF. In addition, the WRF simulation does not reflect the local increase of wind speed. Consequently, the resulting dependence of  $H_5(t)$  with wind forcing from WRF is, on average, lower than that with the wind from the experimental data, and it also does not indicate the peaks. We suppose that the discussed above data assimilation and the LES unit inclusion impact the quality of the WRF output. The same situation as in the case of setting the wind forcing from the experiment is realized for the prediction of the mean wave periods.

The solution for the mean wave period prediction should become the next step of the WAVEWATCH III tuning that includes adjustment to the non-linearity model discussed in subsection "Wind forcing from the experimental data."

## CONCLUSIONS

This paper describes a study of wind-wave regime at the Gorky reservoir. In a series of field experiments, the statistics parameters of wind waves (such as wind speed and direction, temperature stratification of the atmospheric surface layer and of the water column) in the southern part of the reservoir in a wide range of meteorological and hydrological conditions were collected over a four-year period. The basic research of wind flow above the reservoir showed that the values of the drag coefficient  $C_D$  in the range of moderate and strong winds were approximately 50 % lower than its values typical of the ocean conditions. The strong dependence of the retrieved values of the statistical parameters of the wind speed on the height of the wind speed sensors was also shown. In particular, the use of two speed sensors only (the one tracking surface and the adjacent fixed) reduced the scatter in the experimental data significantly, and also rendered lower values. This is due to the specific features of air flow in the reservoir conditions: wind gustiness, stratification of the surface layer, and shielding of wind by banks.

The simulation of surface wind waves on the Gorky reservoir was performed. The wave process was simulated within the tuned WAVEWATCH III model and was calculated both under the influence of unsteady uniform wind field based on the data from the field experiment, and under the wind given by WRF. In the tuned WAVEWATCH III, the new proposed parameterization  $C_D(U_{10})$  suitable for the conditions of a middle-sized reservoir obtained from the series of field experiments was used. The results of the numerical experiments were compared with

the results obtained in the field experiments on the Gorky reservoir.

The uniform unsteady wind speed over the entire water area of the reservoir taken from the field experiment, was in a fairly good agreement with the experiment, but did not describe accurately the case of a highly inhomogeneous wind. Moreover, in the practical prediction of wind and waves, it is necessary to use the numerical models. The accounting for the spatial variability was implemented using WRF. It should be noted, however, that the results should be used with caution, since the horizontal spatial resolution used in the model was the so-called “gray zone”, i.e., the scales which are neither fully sub-grid nor resolved. Under such circumstances, the appearance of artificial large-scale motions resembling convective cells in a real turbulent boundary layer is observed. In [Zilitinkevich et al., 2015] this situation relates to the drawbacks in the simulation of turbulence in the stratified atmosphere (see [Zilitinkevich et al., 2006; Zilitinkevich et al., 2013]).

The results of the WRF application in WAVEWATCH III wind forcing demonstrated the need to improve the simulation within WRF, because the results of the simulation underestimate the value of the wind speed in the considered area and, as a consequence, significant wave height. We suppose that this is due to insufficient accuracy in the topography ( $\approx 1$  km). The wind speed field of ultrahigh spatial resolution can be obtained by incorporating a detailed topography and

inclusion of the LES unit, and by the data assimilation from the experiments and from private weather stations in this area. The prediction of the mean wave periods will be improved with the implementation of the next step of the WAVEWATCH III tuning that includes the adjustment to the non-linearity model.

In addition to the assumptions made in the calculations, the deep water assumption was made. Accounting for the real bathymetry of the Gorky reservoir, as well as the inclusion of the source terms in WAVEWATCH III associated with the transition to shallow water, can make a positive impact on the results.

### ACKNOWLEDGEMENTS

This work was supported by grant of the Government of the Russian Federation (contract 11.G34.31.0048), the RF President’s Grant for Young Scientists (MK-3550.2014.5), and by the RFBR (13-05-00865, 13-05-12093, 14-05-91767, 14-05-31343, 15-35-20953, 15-45-02580). The field experiment was supported by the Russian Science Foundation (Agreement No. 15-17-20009), numerical simulations were partially supported by the Russian Science Foundation (Agreement No. 14-17-00667). We would like to acknowledge high-performance computing support from Yellowstone (ark:/85065/d7wd3xhc) provided by NCAR’s Computational and Information Systems Laboratory, sponsored by the National Science Foundation. ■

### REFERENCES

1. Alves J.-H.G.M., Chawla A., Tolman H.L., Schwab D., Lang G., Mann G. (2011). The Great Lakes Wave Model at NOAA/NCEP: Challenges and Future Developments. //12th International Workshop on Wave Hindcasting and Forecasting, Hawaii.
2. Alves J.-H.G.M., Chawla A., Tolman H.L., Schwab D., Lang G., Mann G. (2014). The Operational Implementation of a Great Lakes Wave Forecasting System at NOAA/NCEP. // Wea. Forecasting, 29, 1473–1497.
3. Atakturk S.S., Katsaros K.B. (1999) Wind Stress and Surface Waves Observed on Lake Washington // Journal of Physical Oceanography, 29, pp. 633–650.

4. Babanin A.V., Makin V.K. (2008) Effects of wind trend and gustiness on the sea drag: Lake George study // *Journal of Geophysical Research*, V.113, C02015, doi:10.1029/2007JC004233.
5. Bakhanov V.V., Bogatov N.A., Ermoshkin A.V., Ivanov A.Y., Lobanov V.N., Kemarskaja O.N., Titov V.I. (2011) Full-scale investigations of the action of internal waves and inhomogeneous currents on the wind waves in the White Sea // *Proc. SPIE 8175, Remote Sensing of the Ocean, Sea Ice, Coastal Waters, and Large Water Regions 2011*, 81750L, doi:10.1117/12.898364.
6. Bogatov N.A., Bakhanov V.V., Ermoshkin A.V., Kazakov V.I., Kemarskaya O.N., Titov V.I., Troitskaya Yu.I. (2014) Using of standard marine radar for determination of a water surface and an atmosphere near-surface layer parameters // *Proc. SPIE 9240, Remote Sensing of the Ocean, Sea Ice, Coastal Waters, and Large Water Regions 2014*, 924013; doi:10.1117/12.2067403.
7. Computational and Information Systems Laboratory. (2012) *Yellowstone: IBM iDataPlex System (University Community Computing)*. Boulder, CO: National Center for Atmospheric Research. <http://n2t.net/ark:/85065/d7wd3xhc>.
8. Donelan M.A., Drennan W.M., Magnusson A.K. (1996) Nonstationary analysis of the directional properties of propagating waves. // *J. Phys. Oceanogr.*, V.26, N.9, P.1901–1914.
9. Fairall C.W., Bradley E.F., Hare J.E. et al. (2003) Bulk Parameterization of Air–Sea Fluxes: Updates and Verification for the COARE Algorithm // *Journal of Climate*, V.16, P.571–591.
10. Gunter H., Hasselmann S., Janssen P.A.E.M. (1992) *The WAM model cycle 4. Technical report No. 4. //DKRZ WAM Model Documentation*. Hamburg. 101 pp.
11. Hasselmann S. and Hasselmann K. (1985) Computations and parameterizations of the nonlinear energy transfer in a gravity-wave spectrum, Part I: A new method for efficient computations of the exact nonlinear transfer integral // *J. Phys. Oceanogr.*, vol. 15, pp. 1369–1377.
12. Hasselmann S., Hasselmann K., Allender J.H., Barnett T.P. (1985) Computations and parameterizations of the nonlinear energy transfer in a gravity-wave spectrum, Part II: parameterizations of nonlinear energy transfer for application in wave models // *J. Phys. Oceanogr.*, vol. 15, pp. 1378–1391.
13. Hesser T.J., Cialone M.A., Anderson M.E. (2013) *Lake St. Clair: Storm Wave and Water Level Modeling*. // The US Army Research and Development Center (ERDC), 156 pp.
14. Ivanov A.V., Troitskaya Yu.I., Papko V.V., Sergeev D.A., Baydakov G.A., Vdovin M.I., Kazakov V.I., Kandaurov A.A., Afanasieva I.M., Donskova O.A., Shuvalova N.M. (2015) Stratifikaciya kak faktor vliyaniya na kachestvo vody na poverkhnosti vodoema (Stratification as a factor of influence on water quality of a plane reservoir) // *Privolzhsky Nauchnyy Journal*, № 34, c.149–156 (In Russian)
15. Kuznetsova A.M., Baydakov G.A., Papko V.V., Kandaurov A.A., Vdovin M.I., Sergeev D.A., Troitskaya Yu. I. (2016) Adjusting of wind input source term in WAVEWATCH III model for the middle-sized water body on the basis of the field experiment. // *Advances in Meteorology*, vol. 2016, Article ID 8539127, 13 pages. doi:10.1155/2016/8539127.



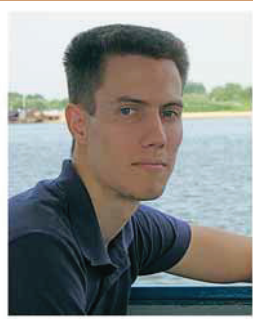
16. Kuznetsova A.M., Baydakov G.A., Papko V.V., Kandaurov A.A., Vdovin M.I., Sergeev D.A., Troitskaya Yu. I. (2016) *Naturnye issledovaniya i chislennoye modelirovaniye vetra i poverkhnostnykh voln na vnutrennikh vodoyemakh srednikh razmerov (Field experiment and simulation of wind and surface waves on the middle-size reservoir)*. // *Meteorologiya i Gidrologiya*, vol. 41, issue 2, pp. 136 – 145 (In Russian).
17. Lopatoukhin L.J., Boukhanovsky A.V., Chernyshova E.S., Ivanov S.V. (2004) *Hindcasting of wind and wave climate of seas around Russia* // *Proc. The 8th International Workshop on Waves Hindcasting and Forecasting, Hawaii*.
18. Poddubnyi S.A., Sukhova E.V. (2002) *Modelirovaniye vliyaniya gidrodinamicheskikh i antropogennykh faktorov na raspredeleniye gidrobiontov v vodokhranilishchakh: Rukovodstvo dlya polzovatelej. (Modeling the effect of hydrodynamical and anthropogenic factors on distribution of hydrobionts in reservoirs: User's Manual)*. // *Institut Biologii Vn. Vod. im. I.D.Papanina*, 116 pp. (In Russian).
19. Sutyrina E.N. (2011) *Opredeleniye kharakteristik volnovogo rezhima Bratskogo vodokhranilishcha (The estimation of characteristics of the Bratskoye Reservoir wave regime)*. // *Izv. Irkutsk State Univ.*, vol.4, 216-226. (In Russian).
20. SWAN team. *SWAN – user manual*. (2006) // *Delft University of Technology, Environmental Fluid Mechanics Section*. 129 pp.
21. Tolman H. and WAVEWATCH III Development Group. *User manual and system documentation of WAVEWATCH III version 4.18*. (2014) // *Environmental Modeling Center, Marine Modeling and Analysis Branch*. 282 pp. + Appendices.
22. Troitskaya Yu. I., Sergeev D.A., Kandaurov A.A., Baidakov G.A., Vdovin M.A., Kazakov V.I. (2012) *Laboratory and theoretical modeling of air-sea momentum transfer under severe wind conditions* // *J. Geophys. Res.*, V.117, Is. C11, C00J21.
23. Wu J. (1982) *Wind-stress coefficients over sea surface from breeze to hurricane* // *J. Geophys. Res.*, vol. 87, pp. 9704–9706.
24. Zilitinkevich S., Kulmala M., Esau I., Baklanov A. (2015) *Megacities – refining models to personal environment*. // *WMO Bulletin* 64 (1), 20–22.
25. Zilitinkevich S.S., Elperin T., Kleerorin N., Rogachevskii I., Esau I.N. (2013) *A hierarchy of energy- and flux-budget (EFB) turbulence closure models for stably stratified geophysical flows*. // *Boundary-Layer Meteorol.* 146, 341–373.
26. Zilitinkevich S.S., Hunt J.C.R., Grachev A.A., Esau I.N., Lalas D.P., Akylas E., Tombrou M., Fairall C.W., Fernando H.J.S., Baklanov A., Joffre S.M. (2006) *The influence of large convective eddies on the surface layer turbulence*. // *Quart. J. Roy. Met. Soc.* 132, 1423–1456.

**Received 01.12.2015**

**Accepted 05.05.2016**



**Alexandra M. Kuznetsova** graduated in 2013 from the Advanced School of General and Applied Physics of Lobachevsky State University (Nizhny Novgorod) with a M.Sc. degree. She then obtained her Ph. D. degree and now works at the Institute of Applied Physics (IAP) of the Russian Academy of Sciences (IAP RAS). Her main interests include atmosphere and hydrosphere, surface layer, planetary boundary layer, simulation, wave models, and atmospheric models.



**Georgy A. Baydakov** graduated from the Radiophysics Department of Lobachevsky State University (Nizhny Novgorod) in 2012. He holds a Ph. D. degree and works at the IAP RAS. The area of his scientific interests includes field investigation of wind-wave interaction and transfer processes in the atmospheric boundary layer and laboratory modeling of the turbulent boundary layer under severe wind conditions.



**Vladislav V. Papko** is Senior Researcher at the Department of Nonlinear Geophysical Processes of the IAP RAS. He graduated from the Radioelectronic Faculty of the Nizhny Novgorod Technical University in 1965. He received his Ph. D. degree (Radiophysics) in the IAP RAS in 1982. His main research interests relate to nonlinear waves, solitons, field experiments, laboratory modeling, and measuring electronic technique. He participated in numerous expeditions to study hydro-physical processes in the ocean. He published nearly 60 scientific papers, including 25 journal articles.



**Alexander A. Kandaurov** graduated from the Advanced School of General and Applied Physics of Lobachevsky State University (Nizhny Novgorod) with a M.Sc. degree in 2011 and received his Ph. D. (physics of atmosphere and hydrosphere) in IAP RAS in 2015. His main research interests are hydrophysics, hydrodynamics measurements, laboratory modeling, and visualization.



**Maxim I. Vdovin** graduated from the Radiophysics Department of Lobachevsky State University of Nizhny Novgorod in 2012. He is Junior Researcher at the IAP RAS. The area of his scientific interests includes wind-wave interactions and transfer processes in the atmospheric boundary layer and laboratory modeling of the turbulent boundary layer under severe wind conditions.



**Daniil A. Sergeev** is Head of the Laboratory of Experimental Methods in Environmental and Technical Hydrodynamics of the IAP RAS. He graduated from the Advanced School of General and Applied Physics of Lobachevsky State University (Nizhny Novgorod) with a M. Sc. degree in 2003 and received his Ph. D. degree (physics of atmosphere and hydrosphere) at the IAP RAS in 2006. His main research interests are physics of atmosphere and ocean boundary layers, hydrodynamics measurements, laboratory modeling, and visualization. He published nearly 100 scientific papers, including 30 journal articles, and made presentations at many international symposiums, conferences, and workshops. He was awarded the Medal of Russian Academy of Sciences in 2009.



**Yuliya I. Troitskaya** is Head of the Department of Nonlinear Geophysical Processes of the IAP RAS. She graduated from the Radiophysics Department of the Lobachevsky State University (Nizhny Novgorod) in 1983. She received her Ph. D. degree (geophysics) at the IAP RAS in 1987 and her D. Sc. degree at the IAP RAS in 1998. Her main research interests are hydrophysics, dynamics of waves, flows and turbulence in the atmosphere and hydrosphere, satellite methods for studying the water surface. She published more than 200 scientific papers, and made presentations at many international symposiums, conferences, and workshops. She was recognized by the Publishing House MAIK-Science for the best publication in 2008. From 1998 to present, she has been Professor of the Advanced School of General and Applied Physics of the Lobachevsky State University (Nizhny Novgorod). She supervised a number of Ph.D. students at the IAP RAS who successfully defended their theses.